

## Direct Probing into the Electrochemical Interface Using a Novel Potential Probe: Au(111) Electrode/NaBF<sub>4</sub> Solution Interface

Dae-Ha Woo, Jung-Suk Yoo, Su-Moon Park,\* Il C. Jeon,<sup>†,\*</sup> and Heon Kang<sup>‡,\*</sup>

Department of Chemistry and Center for Integrated Molecular Systems, Pohang University of Science and Technology, Pohang 790-784, Korea

<sup>†</sup>Department of Chemistry, Jeonbuk National University, Jeonbuk 560-756, Korea

<sup>‡</sup>School of Chemistry, Seoul National University, Seoul 151-742, Korea

Received February 18, 2004

**Key Words :** Electrochemical interface, Electrical double layer, Electrode potential, Scanning tunneling microscopy, Diffuse double layer

In a narrow region of an electrode/electrolyte interface, an electrical double layer (EDL) exists in which ions with an opposite charge to the electrode line up in an excess concentration.<sup>1,2</sup> The EDL is believed to be extremely thin, and the internal electric field strength can exceed 10<sup>7</sup> V/m in routine electrochemical environments. Since its presence was first predicted by theory in the early 20th century,<sup>3-7</sup> understanding of the EDL has been a key to the subjects of practical and fundamental importance such as electrochemistry, corrosion, and the stability of colloidal particles.<sup>8,9</sup>

Numerous experimental approaches have been made to uncover the nature of the EDL. Careful electrochemical studies have measured the interfacial capacitance and the excess charge on electrode surfaces.<sup>7,10</sup> Spectroscopic studies of the vibrational frequency shift of molecules adsorbed on electrode surfaces (vibrational Stark effect) have revealed existence of strong electric fields inside the EDL.<sup>11-14</sup> Real-space investigation of the EDL was first made with a surface force apparatus,<sup>15-18</sup> and then with an atomic force microscope<sup>19-23</sup> by attaching a silica colloidal particle to the tip. These studies measured the electrostatic forces present between EDLs formed at the charged surface and the probe in close distances, from which the thickness of the EDL was deduced. While these studies have greatly contributed to the current understanding of EDLs, many physical aspects still remain in veil for this nanoscopic environment. One of the key features that defines the electrode/electrolyte interface is the electrical potential inside the EDL, but it has not yet been directly measured by experiments and thus far been theoretically predicted<sup>3-7</sup> or deduced from other related physical parameters.<sup>10-23</sup> In this work, we developed a miniaturized probe that can measure the local potential of the solution with subnanometer spatial resolution, and we applied this technique to investigation of the inner potential of electrode/electrolyte interfaces.<sup>24</sup>

The concept of the experimental setup is illustrated in a diagram shown in Figure 1. The electrochemical cell consisted of four electrodes, for which the working electrode (WE) was a flame-annealed Au(111) film deposited on glass, and the counter and reference electrodes (CE and RE) were also gold. If necessary, an Ag/AgCl electrode (in

saturated KCl) was used as an RE for comparison of the observed potentials with the reported values. The electrode potentials were controlled by a bipotentiostat (Pine model AFRDE5). The fourth electrode was a metal probe at its open-circuit potential (ocp). The probe was an electrochemically etched gold wire, coated with a nail polish material except its apex. Aqueous electrolyte solutions were prepared to contain NaBF<sub>4</sub> at various concentrations, which are known to have negligible specific adsorption on a gold surface.<sup>10</sup> The choice of the electrolytes, the gold electrodes, and the probe simplified the electrochemical interface such that it consisted only of the EDL in the absence of specific adsorption of electrolytes or electrochemically active species.

To investigate the interfacial potential the instrument has to meet three requirements: (i) the positioning of a probe inside the EDL formed on an electrode surface with subnanometer spatial precision, (ii) a negligible leakage current through a probe such that it monitors the solution potential without disturbing the local electrolyte concentration, and (iii) a miniaturized probe that can probe into a narrow region of interest with the intended spatial resolution. The first requirement was met by controlling the probe position with a piezo actuator and the control circuit of a scanning tunneling microscope (STM; RHK Technology Inc.). The probe, initially located at the tunneling distance in an STM mode,

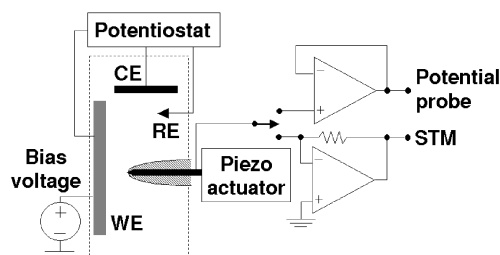


**Figure 1.** Schematic presentation of the apparatus. In an electrochemical cell depicted by the broken-lined box, a potential probe approaches the WE surface and monitors the local potential of the electrochemical interface. The voltage follower accessed by switching from the STM mode reads the potential without passing tunneling currents.

was retracted from the surface to a desired distance far enough to completely escape from the EDL to the bulk ( $> 20$  nm). A potential measurement started from this position, after the probe was switched from the current reading (STM) mode to the voltage monitoring mode. The probe advanced toward the WE surface until a contact was made to the surface, and the voltage read as a function of the distance gave a potential profile of the electrode/electrolyte interface. A complete profiling took 0.1-10 s depending on the probe approach speed, during which the thermal drift of the instrument was negligible ( $< 0.1$  nm/s). To meet the second requirement, the potential was monitored at the probe through a voltage follower circuit with a negligible leakage current (the equilibrium fluctuation current  $\leq 10$  fA at 25 °C). This ensured the probe to read the open-circuit potential of the solution without much destroying the local electrolyte concentration. The third requirement was met by cutting down the height of the bare gold apex of the probe by using the method of ultrashort ( $< 50$  ns) pulse etching,<sup>25</sup> after initial preparation of a probe by insulator coating as mentioned above. The progressive reduction of the gold apex size by the pulse etching produced a gold nano-electrode with a disk-type surface and a small vertical protrusion as monitored by scanning electron microscopy and cyclic voltammetry for the  $\text{Fe}(\text{CN})_6^{3-}/\text{Fe}(\text{CN})_6^{4-}$  redox reaction at the probe.<sup>25</sup> The vertical protrusion of a probe was thought to determine the spatial resolution of a potential profile to be measured, and only the probes that gave the resolution better than a few nm were used.

Results of the potential measurement are shown in Figure 2, in which a gold probe measures the local electrical potential as it approaches the Au(111) surface of the WE in a 1.0 mM  $\text{NaBF}_4$  solution. The different curves correspond to the different bias voltages applied to the WE ( $E_{\text{WE}}$ ) with respect to the gold RE, as marked in the figure. At a sufficiently long distance from the WE surface, indicated as region I, the probe reads a constant potential independent of the probe position. The potential obtained at the probe ( $\phi_{\text{pr}}$ ) in this region is the potential of the solution bulk ( $\phi_{\text{bulk}}$ ) plus the ocp of the probe ( $E_{\text{pr}}^{\text{ocp}}$ ). This value is denoted as  $\phi_{\text{pr}}^0$  in the figure and marked as zero potential in the vertical axis. As the probe approaches the WE surface (region II),  $\phi_{\text{pr}}$  changes gradually toward the potential of the WE ( $\phi_{\text{WE}}$ ). The potential variation in this region reflects the inner potential of the interface. After an electrical contact is made between the probe and the surface (region III),  $\phi_{\text{pr}}$  must be equal to  $\phi_{\text{WE}}$ . The electrical contact point cannot be precisely identified in a  $\phi_{\text{pr}}$  curve because its slope gradually decreases without exhibiting a sharp discontinuity at the contact. Therefore, we measured the mechanical contact point between a probe and the surface by using a distance-modulation technique ( $dI/dz$  measurement)<sup>26</sup> after switching to the STM mode, which is known to provide more accurate determination of the contact position.<sup>27</sup> The mechanical contact position thus identified is located where a  $\phi_{\text{pr}}$  curve just touches the full, constant value of  $\phi_{\text{WE}}$ , and this position is indicated as zero distance in the figure. The result shows that

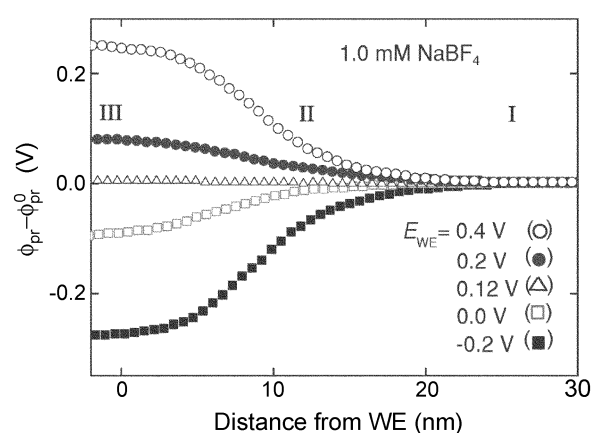


**Figure 2.** The potential measured at the probe as it approaches the Au(111) surface of the WE immersed in a 1.0 mM  $\text{NaBF}_4$  solution. The distance to the bulk is measured from the point of a mechanical contact between the probe and the electrode surface.

a mechanical contact is electrically conducting as well. A few other features of the  $\phi_{\text{pr}}$  curves also need to be mentioned.  $\phi_{\text{WE}}$ , which is the  $\phi_{\text{pr}}$  value measured upon contact to WE, is lower than  $E_{\text{WE}}$  by about 0.12 V, as can be seen from the nearly flat potential profile observed for  $E_{\text{WE}} = 0.12$  V. This potential difference between  $\phi_{\text{WE}}$  and  $E_{\text{WE}}$  must be due to the different ocp values of the WE and the probe, rather than due to specific adsorption of electrolytes. Upon external changes of  $E_{\text{WE}}$ , the  $\phi_{\text{pr}}$  curve is altered only in the vertical direction, such that the value of  $\phi_{\text{pr}} - \phi_{\text{pr}}^0$  scales with  $E_{\text{WE}}$  with an offset of the observed ocp difference of 0.12 V.

The results presented above indicate that the probe reads the local potential of the environment where it is located. This is obvious in region I where  $\phi_{\text{pr}}$  reads the characteristic potential of the solution bulk with an offset of the probe ocp, and in region III where a probe-surface contact is made. Of particular interest is the nature of the  $\phi_{\text{pr}}$  reading in region II. Here the probe is located inside the range of the EDL present on the WE surface. Therefore, the probe must read the inner potential of the EDL, but in this case as well, the potential is read by the probe through the EDL on its own surface. The role that the EDL at the probe plays in potential reading will be discussed in the next paragraph. The  $\phi_{\text{pr}}$  curves show additional features supporting that the probe monitors the interfacial potential. First, the  $\phi_{\text{pr}}$  profiles linearly scale with the applied  $E_{\text{WE}}$  with an offset of the ocp difference (Fig. 2). Second, the thickness of region II becomes narrower as the electrolyte concentration is increased.<sup>1,2</sup> These features also refute experimental artifacts that are possibly involved in the measurements. The linear dependence of  $\phi_{\text{pr}}$  on  $E_{\text{WE}}$  and the symmetric appearance of  $\phi_{\text{pr}}$  profiles with respect to bias polarity suggest that specific adsorption of electrolytes or impurity species does not occur. This statement was verified by additionally performing CV scans of the electrode surfaces and potential measurements in other electrolyte ( $\text{NaClO}_4$  and  $\text{NaF}$ ) solutions. The changing thickness of  $\phi_{\text{pr}}$  profiles with electrolyte concentration denies possibilities of the junction filled with impurities inside a gap between the

probe and the WE, through which  $E_{WE}$  might be leaked to the probe.

In order to interpret the  $\phi_{pr}$  curves quantitatively, it is important to understand how the presence of a probe influences the original EDL at the electrode. The EDL at the probe can interact with the EDL at the WE at close distances. In this case the interfacial potential will result from the two overlapping EDLs, but such EDL overlapping is not well understood and its complete analysis would require extensive theoretical efforts. Here we take a simplified approach for analyzing the  $\phi_{pr}$  curves by introducing the linear superposition approximation (LSA)<sup>28</sup> for the EDL overlapping and assuming that the electrode and the probe both have planar surfaces. The LSA assumes that the interfacial potential from two weakly interacting EDLs is represented as a linear superposition of the potentials of the two independent EDLs. In the present case, the EDL present at WE is due to the charged electrode surface and thus changes with the applied  $E_{WE}$ , whereas the EDL at the probe is due to the ocp of the gold surface and thus unaffected by  $E_{WE}$ . The potential diagram shown in Figure 3 describes the corresponding situation. When an electrode and a probe are far separated (the upper figure), two EDLs exist separately at the WE and probe surfaces (shown as the broken lines). A probe at this distance reads  $E_{pr}^{ocp}$  with respect to  $\phi_{bulk}$ , as mentioned before. As a probe approaches toward a surface (the lower figure), the two EDLs start to overlap, and their potential profiles will be connected smoothly together, as indicated by the solid line in the figure. Within the LSA, if the potential of the EDL at WE is more positive (or negative) than  $\phi_{bulk}$ ,  $\phi_{pr}$  will level up (or down) by this amount upon overlap of the two EDLs. The change of  $\phi_{pr}$  along the approach will therefore trace the potential profile of the EDL at WE. Indeed, in the outer part of region II of the  $\phi_{pr}$  curves where the EDL interaction may be sufficiently weak,  $\phi_{pr}$  appears to follow the exponentially decaying profile of a

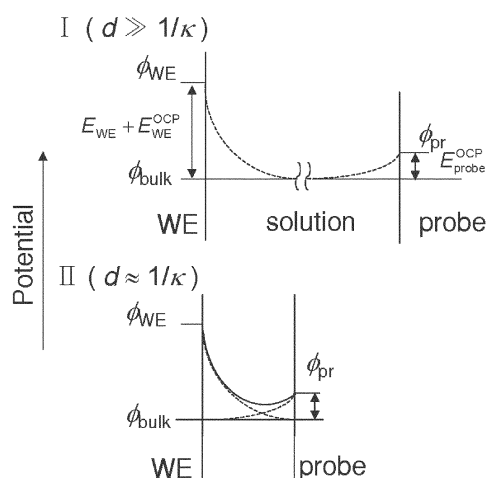


**Figure 3.** Qualitative diagrams of the potential profiles of the EDLs at a WE and at a probe: (I) when a WE and a probe are far separated, and (II) when the two EDLs overlap. The diagrams are drawn for a case of a positive bias at the WE.

diffuse layer of an isolated EDL.<sup>1,2</sup>

Upon further approach of a probe to the WE surface, EDL overlapping will become stronger, and more difficult it will be to justify the LSA analysis.  $\phi_{pr}$  curves in this regime, however, show some interesting features, which at the moment can be addressed only intuitively. Beyond a diffuse layer region,  $\phi_{pr}$  increases approximately linearly toward  $\phi_{WE}$  for some distance and then the curves bend before a probe-surface contact is made. This linear potential region might derive from the Helmholtz plane interfacing with a diffuse layer. Thickness of the linear region increases from about 2 nm at 100 mM to 6 nm at 1 mM. The Helmholtz plane by the original definition would be thinner (about 1 nm thickness), corresponding to two solvent molecules and the radius of the counter ion.<sup>7,10</sup> At low electrolyte concentrations, however, the counter ions are not populated enough, and therefore, the interfacial region of a certain distance from an electrode surface is almost free of ions and this region can basically be regarded as the inner Helmholtz plane. For example, in an electrolyte solution of 1 mM with the ion population of  $1 \times 10^{-3}$  ion/nm<sup>3</sup>, this ion-free region extends to a distance of a few nm from the surface. The linear profile bends slowly toward  $\phi_{WE}$  prior to a surface contact. This behavior might be related to the spillover of the electronic density at a metal surface, which can lead to the electronic density overlapping between the electrode and the probe at a close distance. The jellium model<sup>29</sup> predicts that the electronic spillover occurs over a distance of typically 0.1-0.2 nm, which is too short to rationalize the curve bending over a distance of a few nm. However, STM experiments in electrolyte solutions<sup>27</sup> show that electron tunneling occurs across a distance that is greatly elongated compared to that in vacuum. Such electronic overlapping may affect the potential reading at the probe. We remark again that the above proposals are made on the basis of a rather fragile assumption that the presence of a probe would not significantly affect the potential profile of the EDL. Therefore, credibility of the interpretation remains uncertain. Nonetheless, the interfacial model that is comprised of a jellium electrode, a Helmholtz layer, and a diffuse layer as proposed here, suggests an interesting possibility in that it satisfies the major features of  $\phi_{pr}$  curves and it does not seem to contradict the current understanding of the EDL.

In this work we have demonstrated that the miniaturized potential probe can measure the local potential of the solution and the electrochemical interface with subnanometer spatial resolution. The present result is the first measurement of the interface potential made in real space. The result would stimulate both experimentalists and theorists to further develop new tools for similar measurements as well as relevant theories for a better understanding of the electrified interfaces.

**Acknowledgment.** We thank Professor C. W. Lee for many helpful discussions. This work was supported by Korea Research Foundation (Grant Nos.: 2002-070-C00050 and 2001-DS0035).

## References

1. See, for example, Bard, A. J.; Faulkner, L. R. *Electrochemical Methods*, 2nd Ed.; John Wiley and Sons: New York, 2001; chapter 13.
  2. Schmickler, W. *Interfacial Electrochemistry*; Oxford University Press: Oxford, 1996; chapter 17.
  3. von Helmholtz, H. L. *Wied. Ann.* **1879**, 7, 337.
  4. Gouy, G. *J. Phys.* **1910**, 9, 457.
  5. Chapman, D. L. *Philos. Mag.* **1913**, 25, 475.
  6. Stern, O. *Z. Elektrochem.* **1924**, 30, 508.
  7. Grahame, D. C. *Chem. Rev.* **1947**, 41, 441.
  8. Kim, I. S.; Chon, S. W.; Kim, K. S.; Jeon, I. C. *Bull. Korean Chem. Soc.* **2003**, 24, 1613.
  9. Chang, S.-G.; Lee, H. J.; Kang, H.; Park, S.-M. *Bull. Korean Chem. Soc.* **2001**, 22, 481.
  10. Parsons, R. *Chem. Rev.* **1990**, 90, 813.
  11. Korzeniewski, C.; Shirts, R. B.; Pons, S. *J. Phys. Chem.* **1985**, 89, 2297.
  12. Pope, J. M.; Zheng, T.; Kimbrell, S.; Buttry, D. A. *J. Am. Chem. Soc.* **1992**, 114, 10085.
  13. Zou, S.; Weaver, M. J. *J. Phys. Chem.* **1996**, 100, 4237.
  14. Oklejas, V.; Sjoström, C.; Harris, J. M. *J. Am. Chem. Soc.* **2002**, 124, 2408.
  15. Israelachvili, J. N.; Adams, G. E. *J. Chem. Soc. Faraday Trans. I* **1978**, 74, 975.
  16. (a) Pashley, R. M. *J. Colloid Interface Sci.* **1981**, 83, 531. (b) Israelachvili, J. N.; Pashley, R. M. *Nature* **1983**, 306, 249.
  17. Toprakcioglu, C.; Klein, J.; Luckham, P. F. *J. Chem. Soc. Faraday Trans. I* **1987**, 83, 1703.
  18. Horn, R. G.; Evans, D. F.; Ninham, B. W. *J. Phys. Chem.* **1988**, 92, 3531.
  19. Ducker, W. A.; Senden, T. J.; Pashley, R. M. *Nature* **1991**, 353, 239.
  20. Li, Y. Q.; Tao, N. J.; Pan, J.; Garcia, A. A.; Lindsay, S. M. *Langmuir* **1993**, 9, 637.
  21. Rainovic, Y. I.; Yoon, R. H. *Langmuir* **1994**, 10, 1903.
  22. (a) Hillier, A. C.; Kim, S.; Bard, A. J. *J. Phys. Chem.* **1996**, 100, 18808. (b) Wang, J.; Feldberg, S. W.; Bard, A. J. *J. Phys. Chem. B* **2002**, 106, 10440.
  23. Campbell, S. D.; Hillier, A. C. *Langmuir* **1999**, 15, 891.
  24. Yoo, J. S.; Woo, D.-H.; Bang, K. S.; Park, S.-M.; Jeon, I. C.; Kang, H. *Abstract for the 1st CIMS International Symposium: Nanosciences Related to Electrochemistry*; Postech: Korea, 2001; p 4.
  25. Woo, D.-H.; Kang, H.; Park, S.-M. *Anal. Chem.* **2003**, 75, 6732.
  26. Wiesendanger, R. *Scanning Probe Microscopy and Spectroscopy*; Cambridge University Press: Cambridge, 1994; pp 131-142.
  27. Hong, Y. A.; Hahn, J. R.; Kang, H. *J. Chem. Phys.* **2003**, 119, 10930.
  28. Verwey, E. J. W.; Overbeek, J. Th. G. *Theory of the Stability of Lyophobic Colloids*; Elsevier: Amsterdam, 1948.
  29. Schmickler, W. *Chem. Rev.* **1996**, 96, 3177.
-